Superconductivity of SrAlGe and BaAlGe

Structure and Dynamics of SrAlGeH and BaAlGeH

by

Verina Franika Kranak

A Thesis Presented in Partial Fulfillment
of the Requirement for the Degree
Master of Science

Approved February 2011 by the
Graduate Supervisory Committee:

Ulrich Haussermann, Chair
Dong Kyun Seo
John Kouvetakis

ARIZONA STATE UNIVERSITY

May 2011

ABSTRACT

The discovery of the superconductor MgB_2 led to the increase of research activity for more compounds adopting the AlB_2 structure type and containing superconductive properties. The prominent successor compounds were the silicide systems, AeAlSi (Ae=Sr, Ba, Ca). Presented here is an extension of this investigation to the germanides, SrAlGe and BaAlGe. The ternary structures were synthesized through arc-melting elemental stoichiometric mixtures and structurally characterized by x-ray powder diffraction. Both crystallize as the hexagonal SrPtSb space group (*P* 6*m*2), a variant of the AlB_2 structure type (*P* 6/*mmm*). The low temperature region was measured on a Vibrating Sample Magnetometer (VSM) and both present the onset of superconductivity below 7K.

These compounds are susceptible to hydrogen absorption and the new polyanionic hydrides, SrAlGeH and BaAlGeH, structural and dynamic properties are presented. The hydrides were synthesized via two distinct methods. One method is the reaction of SrH_2 (BaH_2) with elemental mixture of the Al and Ge under pressurized hydrogen and the other is a hydrogenation of the SrAlGe and BaAlGe. Both crystallize in the trigonal SrAlSiH structure type (*P*3*m*1), as determined from Rietveld analysis on powder neutron diffraction measurements. The hydrogen is coordinated by both the active metal and aluminum atoms, providing a unique environment for studying metal-hydrogen interactions.

When exposed to air, both the hydrides and alloys transform from a crystalline grey to an amorphous yellow powder accompanied by a dramatic

volume increase. Infrared spectroscopy shows the disappearance of the bands associated with the Al-H bond and the appearance of Ge-H and O-H bands. This indicates the material reacts with atmospheric water.

ACKNOWLEDGMENTS

I would first like to thank my advisor, Dr. Ulrich Haussermann, for allowing me the opportunity to learn and perform research in solid state chemistry. He has given me unending guidance and encouragement leading me to refine myself as a researcher. In general I would like to acknowledge all of my group members for sharing these years researchof and making them quite enjoyable. Specifically, I would like to thank Dr. Michael Evans for his patience and training in the laboratory and on software programs. I would like to thank Yang Wu for helping me grasp magnetism. I would like to thank Kati Puhakainen for getting me through the tough days of teaching.

I would like to thank Tom Groy for his assistance with X-ray diffraction; Luke Daemon for his assistance with the neutron powder diffraction and inelastic neutron scattering at Los Alamos National Laboratory; and Kenneth Mossman for his assistance and training with the infrared spectroscopy measurements.

I would especially like to thank Jim Bridgewater for his abundant support and care. He made the hard days seem better and the best days more bright. I would like to thank my father for his support, encouragement, conversation and advice. Finally I would like to thank my brother Vaul for reminding me to stay on the lighter side of life.

TABLE OF CONTENTS

Page

LIST OF TABLES

LIST OF FIGURES

Figure Page

1. Introduction

In 2001 MgB_2 was found to superconduct at 39K [1]. This is the highest temperature observed for the onset of superconductivity of intermetallic compounds. MgB_2 adopts the AlB_2 type structure. The boron atoms form graphite like layers and the magnesium atoms are sandwiched between. The report of MgB_2 stimulated the search for more compounds of the same structure type to be tested for superconductive properties. The ternary compounds $Ae(Ga_x,Si_{1-x})_2$ and AeAlSi (Ae = Ca, Sr and Ba) also crystallizes with the AlB_2 structure type [2-4]. Here the alkaline earth metal takes the position of the aluminum atom. The triel and tetrel atoms will share the position of the boron sites as shown in Figure 1 (the terms triel (Tr) and tetrel (Tt) refer to atoms from group 13 and 14 respectively). At the end of 2001 and beginning of 2002, these compounds were investigated for their magnetic properties. Indeed they displayed an onset of superconductivity with the exception of BaAlSi [2-5].

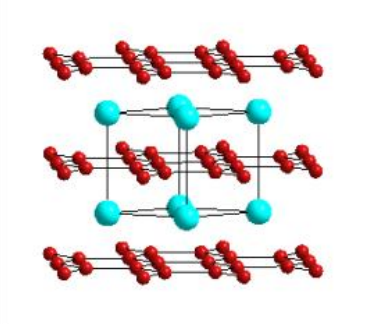

Figure 1. The AlB_2 structure type (Al/Ae – Blue, B/TrTt – Red).

At this time it was proposed that the investigation of these ternary compounds could reveal the mechanism behind the superconductivity in MgB_2 in addition to

perpetuating the search for more ternary AlB_2 type structures that had superconducting properties [2]. However the ternary compounds and MgB_2 are chemically different and therefore the origin of superconductivity should differ. First of all magnesium and boron do not have a significant electronegativity difference resulting in a covalent bonding interaction between the magnesium and the boron nets. This is in contrast to the ternary compounds that have a more polar interaction that causes a substantial electron transfer between the alkaline earth metal and the p-block metal/semi-metal net. Secondly, when counting the number of valence electrons per formula unit, MgB_2 is an 8 electron system whereas the ternary compounds are a 9 electron system. As a consequence the electron-phonon coupling mechanism is different. The MgB_2 has an in-plane vibration coupled to the partially occupied σ-bonding states of the boron atoms [6] and the ternary compounds have an out-of-plane soft mode couple to a partially filled π^* anti-bonding band [7].

The ternary compounds can be considered as Zintl phases. Typical Zintl phase compounds will contain an active metal (alkali, alkaline earth or rare earth metal) and a p-block metal or semi-metal. They are electron precise (valence) compounds which gives rise to semi-conducting or weak conducting properties. Examples of balanced Zintl phases are $SrAl_2$ and $SrGa_2$ [8, 9]. The formal charge transfer between the active metal and the p-block element yields $[Al^-]$ and $[Ga^-]$ ions isoelectronic to a group 14 element. These formal ions form a covalent polyanionic substructure according to their reduced electron configuration. For a 4-valence electron element there are two available geometric nodes; either a

tetrahedral (sp^3) or a trigonal planar (sp^2) coordination. The tetrahedral node forms 4 σ-bonds satisfying the octet-rule and building a diamond like substructure and variations therein, as shown in $SrAl_2$ (Figure 2). The trigonal planar node forms 3 σ-bonds to yield a graphitic layer as shown in $SrGa_2$ (Figure 1). There in the singly-occupied p-orbital forms a π-bonding and antibonding band, of which the bonding band is filled. The electronic bonding in $SrGa_2$ illustrates the same picture where three σ-bonding bands arising from the σ bonding interaction between each gallium (s, p_x, p_y) and one π-bonding band (p_z) filled [9].

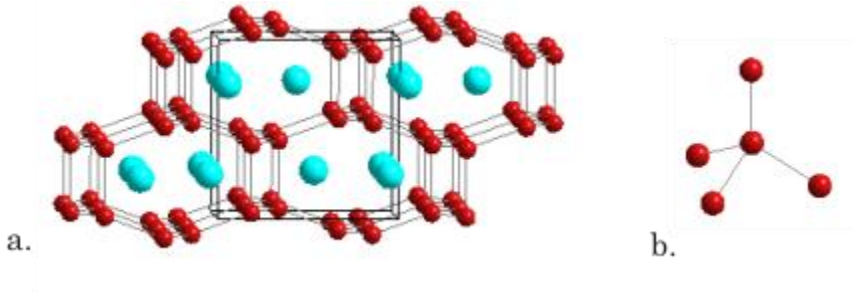

Figure 2. (a) Orthorhombic $SrAl_2$ (Sr – Blue, Al – Red). (b) The tetrahedral node that builds the covalent polyanionic substructure.

In the ternary AlB_2 compounds one group 13 atom is replaced with one group 14 atom (ie SrAlSi). This introduces an additional electron which goes into the π^* antibonding band (Figure 3) [10]. These systems are therefore no longer electron precise and deemed imbalanced Zintl Phases, a rare occurrence. The compensation for this peculiarity of 9 electron compounds is where the unusual properties arise. One consequence of the imbalance is the occurrence of superconductivity [7, 10]. Another is the puckering of the hexagon layers [11, 12]. A puckered variation on the AlB_2 type structure is the YPtAs structure type

(Figure 4) [13]. The pronounced puckering demonstrated here eliminates the p_z π-bonding interaction and leads to a more localized lone pair electronic states [11]. This is observed for the Sn compounds (e.g. SrGaSn) [11, 14]. In the severe puckering case no superconductivity is observed [11].

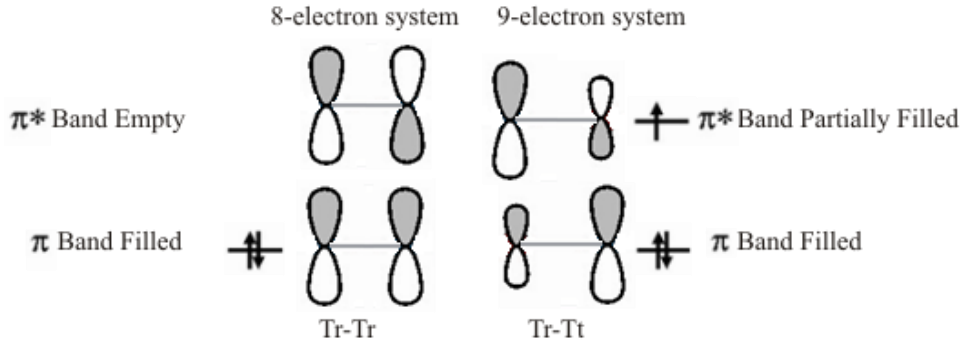

Figure 3. Illustration comparing the π-bonding and π^*-antibonding bands of the 8 and 9 electron systems.

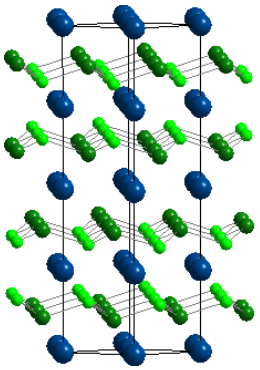

Figure 4. Puckered hexagon nets in SrGaSn (YPtSb- type; space group *P* 6_3*mmc;* Sr – Blue, Ga – light green, Sn – dark green).

While this exploration of the 9 electron AeTrTt has been thoroughly performed for the silicides and partially for the stannides it has not been extended to the germanides. Herein is the investigation of the magnetic properties at low temperatures for BaAlGe and SrAlGe.

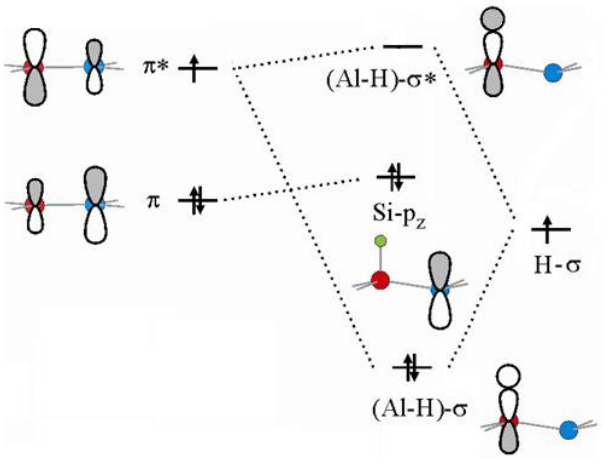

Figure 5. Illustration of the π bonding and π^* antibonding bands energy level change upon the addition of hydrogen for SrAlSiH. Illustration modified with permission from reference 15.

Another property of these imbalanced Zintl phases is their susceptibility to hydrogenation, previously seen in SrAlSiH [15]. The more electropositive triel contributes more to the π^* anti-bonding band (Figure 5). Thus the hydrogen will bond to the triel creating a filled σ-bonding band at a much lower energy and the silicon p_z orbital becomes non-bonding with one lone-pair at a slightly higher energy. The overall electron count increases to 10 and the compound is electron precise exhibiting the properties of a semi-conductor or weak conductor as defined by the Zintl-Klemm concept. Therefore SrAlGe and BaAlGe are also examined for their reactivity to hydrogen.

2. Experimental Methods

2.1. Synthesis

All steps of synthesis and sample preparation were carried out in an Ar-filled glove box. Sr (99.9% purity) and Ge (99.999% purity) were purchased from Alfa Aesar; Ba (99.99%) and Al (99.99%) were purchased from Sigma-Aldrich. The compounds SrAlGe and BaAlGe were prepared by arc-melting stoichiometric amounts of the pure elements. SrAlGeH and BaAlGeH were synthesized by two different methods. The first method for synthesizing SrAlGeH and BaAlGeH involved a direct reaction of hydrogen with ternary precursors SrAlGe and BaAlGe, respectively. The precursor powders were pressed into pellets, placed into corundum crucibles, and loaded into stainless steel autoclaves. Reactions were carried out at 400 °C for 72 h and a hydrogen pressure of 80 bar.

The second method was an indirect synthesis from the elements (Al and Ge) and an alkaline earth hydride. SrH_2 and BaH_2 were made by placing elemental Sr/Ba into a corundum crucible, which was loaded into a stainless steel autoclave and reacted with 30 bar of H_2 at 750 °C for 4 h. Stoichiometric amounts of Al, Ge, and alkaline earth hydride were pressed into a pellet and placed in a corundum crucible, which was heated at 650 °C for 24 h in the presence of 50 bar H_2. The sample was then ground, pressed again into a pellet, returned to the autoclave and heated to 750 °C for 24 h at 50 bar H_2. This procedure was repeated 3-4 more times to achieve a homogenous and single phase product. The deuterides were prepared analogously. The phase purity of starting materials, hydrides and

deuterides was established by X-ray diffraction (Siemens D5000 diffractometer; Bragg Brentano geometry; Cu Kα radiation).

2.2. Structure characterization

Lattice parameters of the ternary intermetallics SrAlGe and BaAlGe, and their hydrides and deuterides were obtained from least-squares refinement of the measured and indexed lines of the corresponding powder diffractograms [PIRUM] [16]. Atomic Positions of SrAlGeD and BaAlGeD were determined by Rietveld analysis [17] of neutron powder diffraction data using the programs GSAS [18] and EXPGUI [19]. Time-of-flight neutron diffraction data were measured on the neutron diffraction data were measured on the neutron powder diffractometer (NPDF) at the Lujan Neutron Scattering Center at Los Alamos National Laboratory [20]. Each sample (about 3.0 g) was loaded into sealed vanadium canisters and measured at room temperature. For the Rietveld refinement (Figure 8) initial values for the atomic coordinates were taken from computationally relaxed structural parameters obtained from first principle calculations. Unit cell, scale factor and zero correction were refined first, and the background was fit graphically and bootstrapped. Atomic coordinates, U_{iso} then background were refined. A second phase ($SrAl_2Ge_2$) was added to SrAlGeD, and its unit cell was refined. At this point, the profile was fitted with profile function 4. During profile refinement all other parameters were turned off, except scale factor. Once the profile was adequately modeled, the other parameters were turned on in this order: background, unit cell, zero, atomic coordinates, U_{iso}. For

SrAlGeD, U_{iso} of Sr had to be refined separately as it caused the refinement to diverge.

2.3. Magnetization measurements

Temperature-dependent magnetization (Figure 7) of the ternary precursors BaAlGe and SrAlGe were measured by Vibrating Sample Magnetometer (VSM) on a Quantum Design PPMS system. Specimens were prepared by pressing 20-80mg of powdered sample into a tablet which was placed in a brass trough sample holder with a small amount of fast-curing superglue. These steps were performed under dry argon and the sample holder was loaded vertically into the PPMS chamber. The temperature was scanned from 15K to 2K at a rate of 0.1K/min.

2.4. Spectroscopic investigation

Inelastic Neutron Scattering (INS) spectroscopy was performed on the filter difference spectrometer (FDS) instrument at the Lujan Center at Los Alamos National Laboratory. SrAlGeH and BaAlGeH samples (about 3 g) were loaded into an aluminum sample holder under a He atmosphere. The sample holder was subsequently sealed and mounted in a cryostat. The spectra of the two hydrides were measured at 10 K (Figure 10). Data were treated by discrete, direct deconvolution of the instrument resolution function [21-23], which provides an energy resolution on the order of 4-5%.

Fourier-transform Infrared Spectroscopy (FT-IR) investigations of the hydrides were performed on a Bruker IFS 66v/s instrument (Figure 12). KBr pellets were prepared in Ar-filled glove box.

3. Results and Discussion

3.1. Crystal Structure of AeAlGe

The AeAlSi (Ae = Sr, Ba, Ca) structures have been thoroughly investigated. They adopt the AlB_2 type structure (space group *P* 6/*mmm*). The alkaline earth atom occupies the corners of the unit cell (Wyckoff site 1*a*) and the TrTt atoms occupy the trigonal prismatic sites (Wyckoff site 2*d*) forming a two-dimensional graphite-like layer [13]. The cell parameters of the silicides change upon the exchange of the alkali earth metal (Table 1). Going from the smaller calcium to the larger barium the *a* cell parameter in the silicides experiences a small increase (4.189Å – 4.290Å). However the *c* parameter, the stacking direction of the hexagon nets, increases significantly (4.400Å – 5.140Å).

Table 1
Lattice Parameters of AeAlTt (Ae=Ca, Sr, Ba; Tt=Al, Si), Interatomic Distances of Al – Tt and Superconductor Transition Temperatures.

Compounds	CaAlSi	SrAlSi	BaAlSi	SrAlGe	BaAlGe
a (Å)	4.189 [a]	4.220 [a]	4.290 [a]	4.304 [c]	4.315 [c]
c (Å)	4.400 [a]	4.754 [a]	5.140 [a]	4.741 [c]	5.140 [c]
d [Al-Tt (Å)]	2.420 [b]	2.446 [b]	2.484 [b]	2.479 [d]	2.511 [e]
T_c (K)	7.8 [a]	5.1 [a]	< 2 [a]	6.7 [c]	6.3 [c]

[a] [Reference 4]; [b] [Reference 15]; [c] [Reference 11]; [d] [Reference 24]; [e] [Reference 25]

In contrast to the silicon system AeAlGe does not afford the calcium compound CaAlGe. When comparing the SrAlGe and BaAlGe to SrAlSi and BaAlSi, respectively, the *c* parameter changes very little (≥0.01Å). However the *a* parameter which is affected by the size of the hexagon rings increases due the

larger germanium (Table 1). Previous characterization has shown that these two compounds adopt the SrPtSb type structure (space group *P* 6*m*2, Figure 6) [24, 25]. This is a lower symmetry variant of the AlB_2 type [13]. Here each planar hexagon is comprised of two 1-fold Wyckoff sites which will allow for ordering of the Tr and Tt atoms.

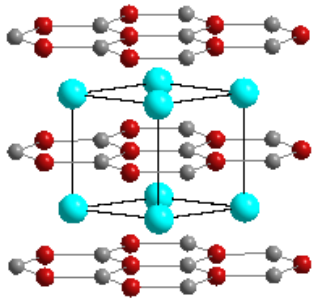

Figure 6. Illustration of BaAlGe (SrPtSb-type structure; space group *P* 6*m*2; Ba – blue, Al – red, Ge – grey).

3.2. Magnetic measurements of AeAlGe

Low temperature magnetic measurements for SrAlGe and BaAlGe showed a T_c of 6.7K and 6.3K respectively (Table 1) [11]. Overall the T_c of the germanides is higher in comparison to their silicide counterparts. From this it may be speculated that if CaAlGe was synthetically obtainable it may have a higher T_c than CaAlSi.

One notable T_c trend shared in both the silicide and germanide systems is observed upon changing the alkali earth metal. When the active metal is replaced with a smaller active metal the T_c increases [7].

Further analysis of the superconductive properties beyond the determination of transition temperature of the germanide systems was conducted. Both field cooled (FC) and zero field cooled (ZFC) techniques were used to identify if these materials were bulk superconductors (Figure 7). The magnetic shielding fraction in the ZFC measurement is greater than 90% of the theoretical value for a perfect diamagnet (1/4π) at 2K for both compounds (crystallographic densities of SrAlGe and BaAlGe are 4.011 and 4.618 g/cm^3) [11]. The flux exclusion in the FC measurement is about 50% and 10% at 2K for BaAlGe and SrAlGe, respectively. This information identifies both compounds as being bulk superconductors.

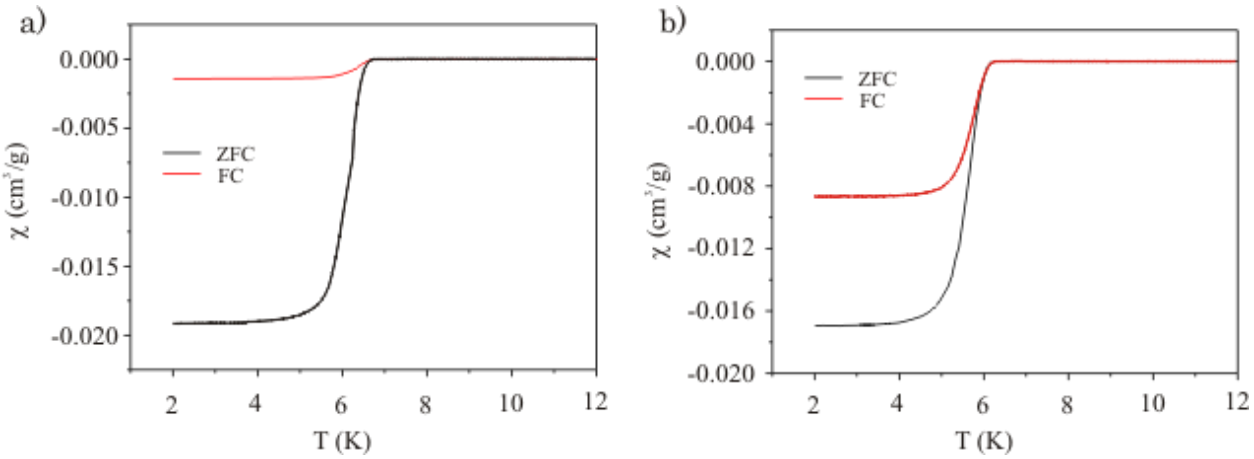

Figure 7. Susceptibility of (a) SrAlGe and (b) BaAlGe at 10 Oe as a function of temperature (zero-field cooling ZFC, field cooling FC) [12].

In conclusion, superconductivity is shown here to be extended to the germanides. The arrangement of the group 13 and 14 atoms in either a disordered (i.e. AlB_2) or ordered (i.e. SrPtSb) manner showed no significant effect on the proclivity toward superconductive properties. The underlying similarities to the

silicide system are the imbalanced number of valence electrons per formula unit and the superficial structure of AlB_2.

3.3. Crystal Structure of AeAlGeH

The electronically imbalanced Zintl phases are susceptible to the addition of hydrogen. The resulting $[AlGeH]^{2-}$ polyanion is electron precise. The new 10-electron quaternary system is an opportunity to study the bonding properties of hydrogen compared with $[AlSiH]^{2-}$ and other hydrides within the polyanionic hydrides AeTrTtH system that incorporate different alkali earth metals and tetrels.

The structure of BaAlGeD and SrAlGeD was confirmed by Rietveld analysis from neutron powder diffraction (Figure 7) [26]. Both structures crystallize with the trigonal SrAlSiH-type structure (space group *P* 3*m*1; Figure 8; Tables 2 and 3). The hydrogen induces a slight puckering of the hexagon layers accompanied with a small increase in the c/*a* ratio. Those layers are stacked on top of each other in the same orientation. The Al (Wyckoff site 1*c*) and Ge (Wyckoff site 1*b*) atoms maintain the same ordering in the hexagon as the precursor. The alkaline earth atom (Wyckoff site 1a) maintains the same position relative to the hexagon layer as the precursor. The interatomic distances for these compounds are given in Table 4. The Al-Ge distance increases very slightly from the precursor to the hydride; a change of 0.036Å and 0.015Å for the Ba and Sr compounds respectively. The Al-H terminal bond, 1.73 – 1.74 Å, is longer than the Al-H terminal bond in molecular species AlH_n (n = 1,2,3) or solid state alane and alanates (1.57Å – 1.64Å) [27]. This observed bond length is consistent with

the AeAlSiH compounds [15]. The Ae-H interatomic distance in SrAlGeH and BaAlGeH corresponds well to the Ae-H distances in the binary salts MH_2 [28, 29].

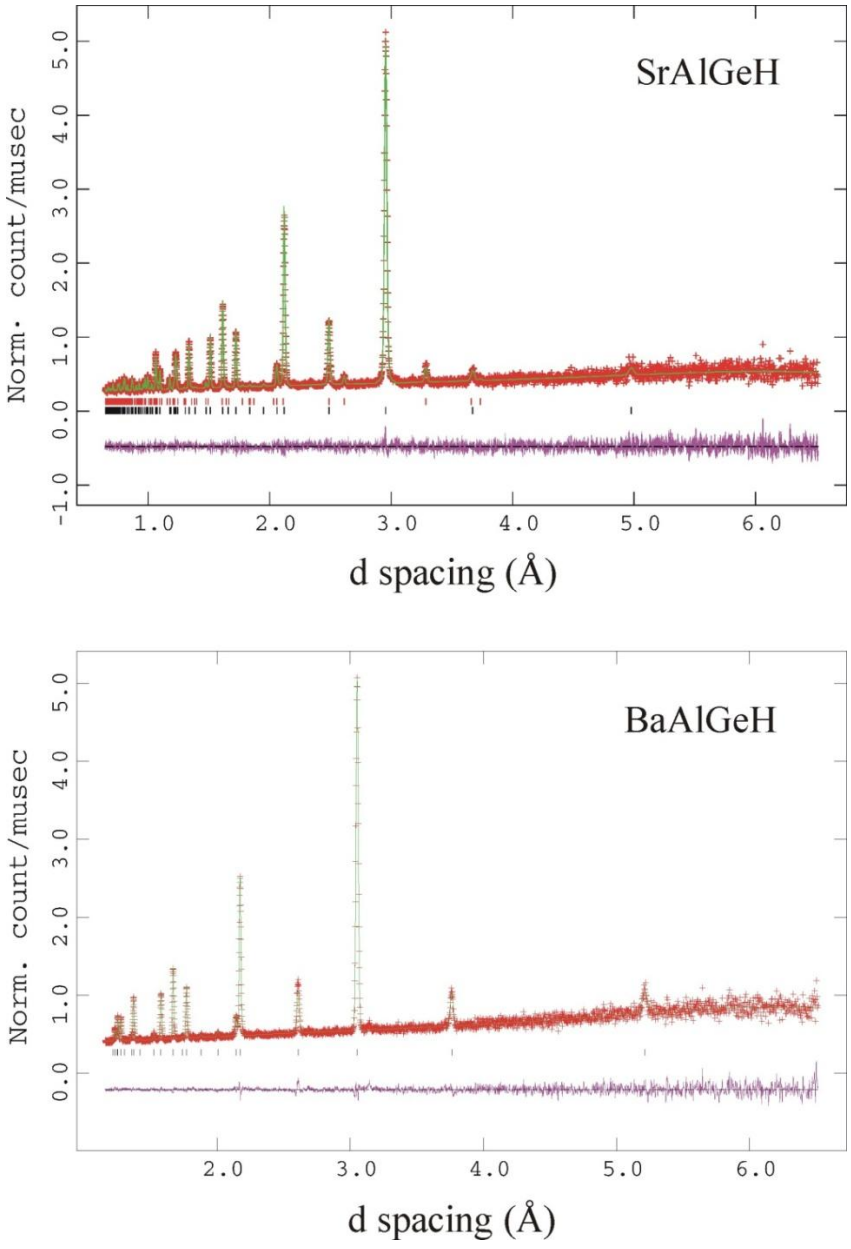

Figure 8. Rietveld fit to the neutron powder diffraction of SrAlGeD and BaAlGeD. Crosses represent the observed pattern and the solid line is the calculated pattern. Bragg positions are indicated by vertical markers. The impurity phase in SrAlGeD pattern is $SrAl_2Ge_2$ [26].

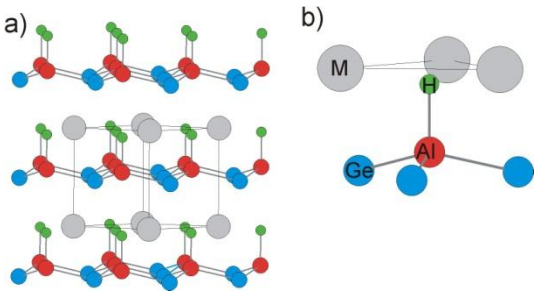

Figure 9. (a) The trigonal structure of AeAlGeH (M – Grey, Al – Red, Ge – Blue, H – Green). (b) Tetrahedral coordination environment of H by three Ae and one Al atoms

Table 2.
Crystal Data and structure refinement of AeAlGeD.[a]

Compound	BaAlGeD	SrAlGeD
Space Group	*P*3*m*1	*P*3*m*1
Z	1	1
a, (Å)	4.3444(4)	4.2421(6)
c, (Å)	5.2115(7)	4.9691(9)
c/*a*	1.20	1.17
V	85.18(1)	77.44(1)
Temp, K	295	295
Chi^2	2.596	3.159
Rp, %	1.32	1.83
Rwp, %	1.89	2.58

[a] Lattice parameters from X-ray data

Table 3.
Atomic coordinates, isotropic displacement parameters (Å^2), and site occupancies for AeAlGeD (SG *P* 3*m*1).

Atom	Wyckoff position	X	y	Z	U_{eq}	occ.
Ba	1a	0	0	0	0.0024(2)	1
Al	1c	2/3	1/3	0.5395(5)	0.0118(4)	1
Ge	1b	1/3	2/3	0.4551(4)	0.0125(2)	1
D	1c	2/3	1/3	0.8703(4)	0.0148(3)	1
Sr	1a	0	0	0	0.0085(5)	1
Al	1c	2/3	1/3	0.5363(6)	0.0068(8)	1
Ge	1b	1/3	2/3	0.4418(6)	0.0119(2)	1
D	1c	2/3	1/3	0.8864(5)	0.0230(9)	1

Table 4.
Selected Interatomic Distances (Å) and Angles (^{o}) in AeAlGeD.

Compound	BaAlGeD	SrAlGeD
Ae-D	2.598(1)	2.513(1)
Al-D	1.725(3)	1.742(4)
Al-Ge	2.547(1)	2.494(1)
Al-Ge-Al	117.08(7)	116.53(9)
Ge-Al-D	99.95(8)	100.87(10)
Torsion	33.3(1)	36.2(1)

3.4. Vibrational properties of AeAlGe

Inelastic neutron scattering (INS) was performed on both hydrides to further characterize the strength of the Al-H and Ae-H bonding interactions. The INS spectra show two bands around 900 and 1250cm^{-1} corresponding to the bending and stretching modes of Al-H respectively (Figure 10) [26]. The identity of these bands is verified by previously calculated phonon dispersions along special directions in the hexagonal Brillouin zone [26]. This curve shows that the bending mode is degenerate and therefore will display a higher intensity in the INS spectrum.

The stretching mode is a direct measurement of the strength of the Al-H bond because the hydrogen is terminally bonded to the aluminum. The Al-H stretches in the AeAlTtH systems are typically found in the range of 1200-1250 cm^{-1}. SrAlSiH and BaAlSiH are found around 1220cm^{-1} and 1240 cm^{-1} respectively [15, 30], a much lower frequency than those found in molecular alanates at 1682-1882 cm^{-1}[27]. This suggests that the Al-H bond is quite weak, which is also supported by the longer bond length.

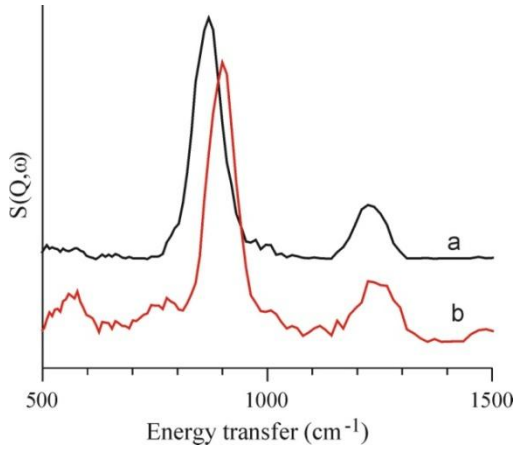

Figure 10. INS spectrum of (a) SrAlGeH and (b) BaAlGeH [26].

The covalent Al-H bond can be thought of as a dative bond where the hydrogen adds hydridically to the aluminum atom of which already has three bonds and a zero formal charge (Figure 11b) [15]. Then the metal, forming an ionic interaction with the hydride, pulls the hydrogen from the aluminum lengthening the Al-H bond.

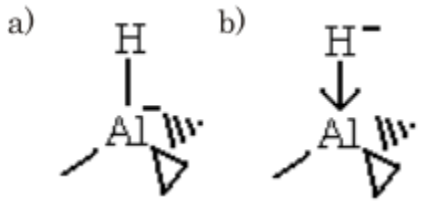

Figure 11. An illustration of the border cases of the Al-H bond. (a) Illustrates the Al-H bond arising from shared electrons. (b) Illustrates a dative bond assuming the hydrogen is hydridic.

The movement of the hydrogen displacing toward the alkali earth atom is shown in the bending mode and therefore an indirect measurement of the Ae-H interaction strength. As expected this frequency has a more pronounced shift to a

lower frequency as the lighter strontium replaces the heavier barium [26]. The meaning of which is that barium forms a stronger interaction with the hydrogen.

3.5. Thermal behavior of AeAlGe

The high synthesis temperature, above 700 °C, illustrates the thermal stability of the hydrogenated aluminum germanides. This translates to high desorption temperatures. BaAlGeH and SrAlGeH are found to desorb hydrogen around 500 °C and 530 °C, respectively, under dynamic vacuum condition of (10^{-4} torr). This is similar to BaAlSiH and SrAlSiH, which decompose above 600 °C under isochoric conditions and above 500 °C under dynamic vacuum conditions [15, 31].

The decomposition of both SrAlSiH and BaAlSiH yields quantitatively the underlying AlB_2-type alloys [15, 31]. While this is true of BaAlGeH, SrAlGeH results in the AlB_2-type alloy along with additional reflections in the X-ray diffraction pattern suggesting further decomposition under the applied conditions.

3.6. Moisture induced decomposition

While thermally rather stable, the hydrides SrAlGeH and BaAlGeH are highly moisture sensitive. After short exposure to air they transform from grey crystalline into colored amorphous materials. This behavior is radically different from SrAlSiH and BaAlSiH which can be kept in air, and even in water, without degradation [15, 31]. Figure 12 displays a sequence of IR spectra showing the decomposition of SrAlGeH [26]. The material was exposed to air for the given

durations of time before being pressed into a KBr pellet. The KBr pellet was prepared and brought to the spectrometer under moisture-free conditions. The initial spectrum shows the two bands associated with the Al-H stretch and bending mode, around 1220 and 900 cm^{-1}, respectively, in agreement with the INS investigations.

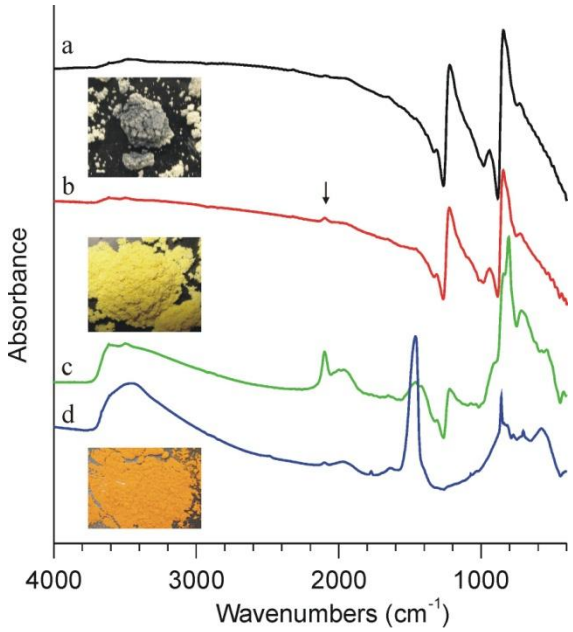

Figure 12. Infrared spectra of a SrAlGeH sample exposed to air for 0 min (a), 4 min (b), 12 min (c), and one year (d). The photographs show the colos of the materials b-d. The arrow in the spectrum (b) marks the onset of the Ge-H stretch [26].

After four minutes an additional peak at 2100 cm^{-1} starts to appear, which is well pronounced in the spectrum taken after 12 minutes. This peak is assigned to a Ge-H stretching vibration. Accordingly a Ge-H bending mode is expected at around 550-600 cm^{-1}. The broad band around 3500 cm-1 is typical for O-H stretches. Additional broad bands are visible around 2000 and 1500 cm^{-1}. The latter may correspond to O-H bending modes. The Al-H bands of the original

material have basically disappeared. The low frequency region (600 – 900 cm^{-1}) exhibits new features, which can be associated with Al-O and/or Ge-O stretching modes. This experiment indicates that when exposing AeAlGeH to moisture, Al-H entities in the initial hydride change presumably into Al-O(H) while Ge atoms attain a H ligand. It is not clear if the original Al-Ge hexagon layer is still present or broken up by O. The complete amorphization of the hydride material points to the latter scenario. In topotactic reactions of isoelectronic $CaGe_2$ - consisting of corrugated hexagon layers formed by Ge atoms - to polygermyne, $(GeH)_n$, crystallinity is maintained to a large extent. Interestingly, the IR spectrum of the sample exposed to air for 12 minutes resembles the one of polygermyne in terms of the Ge-H features [32]. The final product of moisture decomposed SrAlGeH or BaAlGeH has an orange color. The IR spectrum is characterized by a sharp band at 1500 cm^{-1}. The Ge-H stretch is absent.

4. Conclusions

The imbalanced Zintl phases of CaAlSi and SrAlSi containing the AlB_2 structure type have previously been shown to superconduct. This investigation has now been extended to SrAlGe and BaAlGe (CaAlGe could not be synthesized). While both the silicide and germanide compounds are imbalanced Zintl phases, the latter is of the SrPtSb structure type, an ordered variant of the AlB_2 structure-type.

The imbalanced Zintl phases are susceptible to the addition of hydrogen. The inclusion of hydrogen produces a favorable 10-electron (electron precise) system. This has already been shown for SrAlSiH, an air and moisture stable compound. The hydrogen covalently bonds to the aluminum and forms an ionic interaction by three coordinating metals. The strength of both the covalent bond and the ionic interaction are indicated through Inelastic Neutron Scattering.

The current research presents the new compounds SrAlGeH and BaAlGeH. Both form the trigonal SrAlSiH structure type, space group *P*3*m*1. The low frequency of the Al-H stretching mode found in the INS spectra indicates a weak bond, and does not vary with changing either metal or the group 14 element. The frequency of the Al-H bending mode increases with the heavier metals suggesting that the ionic interaction of the hydrogen increases from strontium to barium.

Unlike SrAlSiH, these compounds are not air and moisture stable. When exposed to air the compounds progressively turn from grey to yellow to orange accompanied by an increase in volume. IR spectra indicate the loss of Al-H bonds and the introduction of O-H stretching and bending modes. It appears that Ge-H

and Al-O(H) bonds and peaks associated with Al-O and Ge-O appear. Although it is not clear if the hexagonal layers are maintained or broken up by oxygen, x-ray diffraction patterns indicate amorphization.

Common among the AeAlTt compounds is the high reaction temperature and the corresponding thermal stability. Decomposition occurs at 500˚C under dynamic vacuum conditions for both SrAlSiH and BaAlGeH, and at 530˚C for SrAlGeH. The decomposition releases the hydrogen and the original ternary SrPtSb structure is maintained. Additional peaks are present in the x-ray diffraction patterns of SrAlGe after decomposition from SrAlGeH indicating possible further decomposition.

References

1. J. Nagamatsu, N. Nakagawa, T. Muranaka, Y. Zenitani, J. Akimitsu, Nature 410 (2001) 63-64.

2. M. Imai, K. Nishida, T. Kimura, H. Abe, Physica C 377 (2002) 96-100.

3. M. Imai, K. Nishida, T. Kimura, H. Abe, Appl.Phys. Lett. 80 2002 1019-1021.

4. B. Lorenz, J. Lenzi, J. Cmaidalka, R. Meng, Y. Sung, Y. Xue, C. Chu, Physica C 383 (2002) 191-196.

5. S. Yamanaka, T. Otsuki, T. Ide, H. Fukuoka, R. Kumashiro, T. Rachi, K. Tanigaki, F. Guo, K. Kobayashi, Physica C 451 (2007) 19-23.

6. H. Choi, D. Roundy, H. Sun, M. Cohen, S. Louie, Nature 418 (2002) 758-760.

7. R. Heid, K. Bohnen, B. Renker, P. Adelmann, T. Wolf, D. Ernst, H. Schober, J. Low Temp. Phys. 147 (2007) 375-386.

8. G. Nagorsen, H. Posch, H. Sch*a*fer, A. Weiss, Z. Naturforchg. 24b (1969) 1191.

9. F. Haarmann, K. Koch, D. Gr*u*ner, W. Schnelle, O. Pecher, R. Cardoso-Gil, H. Borrmann, H. Rosner, Y. Grin, Chem. Eur. J. 15 (2009) 1673-1684.

10. M. Giantomassi, L. Boeri, and G. B. Bachelet, Phys. Rev. B (2005) 72 224512.

11. M. Evans, Y. Wu, V. Kranak, N. Newman, A. Reller, F. Garcia-Garcia, U. Haussermann, Phys Rev. B 80 (2009) 064514.

12. K. Sparta, R. M*u*ller, M. Merz, G. Roth, P. Adelmann, T. Wolf, Acta Cryst. B62 (2006) 710-718.

13. R. Hoffmann, R. P*o*ttgen, Z. Kristallogr. 216 (2001) 127-145.

14. A. Czybulka, B. Pinger, and H. Schuster, Z. Anorg. Allg. Chem. 579 (1989) 151-157.

15. M. Lee, T. Björling, B. Hauback, T. Utsumi, D. Moser, D. Bull, D. Noréus, O. Sankey, U. Häussermann, Phys Rev. B 78 (2008) 195209.

16. P. Werner, Arkiv foer Kemi 31 (1969) 513-516.

17. R. A. Young, Ed. The Rietveld Method, Vol. 5 Oxford Universtiy Press: New York, 1995.

18. A. C. Larson, R. B. von Dreele, General Structure Analysis System *(GSAS)*, Los Alamos National Laboratory Report LAUR 86-748, 2004.

19. B. H. Toby, J. Appl. Cryst. 34 (2001) 210-213.

20. T. Proffen, T. Egami, S.J.L. Billinge, A.K. Cheetham, D. Louca, J.B. Parise, Appl. Phys. A 74 (2002) S163-S165.

21. A.D. Taylor, E.J. Wood, J.A.Goldstone, J. Eckert, Nucl. Inst. Meth. Phys. Res. 221 (1994) 408.

22. F. Mezei, P.Vorderwisch, Physica B 156 (1989) 678-680.

23. E.I. Litvinenko, E.P. Zhidkov, Comp. Phys. Comm. 127 (2000) 229.

24. B. Eisenmann, M. Rhode, M Wendorff, C. R*o*hr, Z. Anorg. Allg. Chem. 634 (2008) 153-165.

25. M. Wendorff, C. R*o*hr, Z. Naturforsch. 62b (2007) 1059-1070.

26. V. Kranak, M. Evans, L. Daemen, T Proffen, M. Lee, O. Sankey, U. Haussermann, Solid State Sci. 11 (2009) 1847-1853.

27. S. Aldridge, A.J. Downs, Chem. Rev. 101 (2001) 3305-3365.

28. T. Sichla and H. Jacobs, Eur. J. Sol. State Inor. 33 (1996) 453

29. W. Bronger, C. S. Chi, and P. Mueller, Z. Anorg. Allg. Chem. 545 (1987) 69.

30. M. Lee, O. Sankey, T. Bj*o*rling, D. Moser, D. Nor*e*us, S. Parker, U. Haussermann, Inorg. Chem. 46 (2007) 6987-6991.

31. T. Bj*o*rling, D. Nor*e*us, K. Jansson, M. Andersson, E. Leonova, M. Eld*e*n, U. H*a*lenius, U. Haussermann, Angew. Chemi. Int. Ed. 44 (2005) 7269-7273.

32. G. Vogg, G, M. Brandt, M. Stutzmann, Adv. Mat. 12 (2000) 1278-1281.